

 Open access • Journal Article • DOI:10.1109/TPWRS.2013.2272494

Analysis of Power Sharing and Voltage Deviations in Droop-Controlled DC Grids

— [Source link](#) 

Jef Beerten, Ronnie Belmans





Institutions: Katholieke Universiteit Leuven

Published on: 20 Aug 2013 - IEEE Transactions on Power Systems (IEEE)

Topics: Voltage droop, Forward converter, Cuk converter, Flyback converter and Boost converter

Related papers:

- [Impact of DC Line Voltage Drops on Power Flow of MTDC Using Droop Control](#)
- [Adaptive Droop Control for Effective Power Sharing in Multi-Terminal DC \(MTDC\) Grids](#)
- [Methodology for Droop Control Dynamic Analysis of Multiterminal VSC-HVDC Grids for Offshore Wind Farms](#)
- [A Generalized Voltage Droop Strategy for Control of Multiterminal DC Grids](#)
- [An Improved Droop Control Method for DC Microgrids Based on Low Bandwidth Communication With DC Bus Voltage Restoration and Enhanced Current Sharing Accuracy](#)

Share this paper:    

View more about this paper here: <https://typeset.io/papers/analysis-of-power-sharing-and-voltage-deviations-in-droop-1dxssep1gw>

J. Beerten and R. Belmans, "Analysis of power sharing and voltage deviations in droop-controlled DC grids," *IEEE Transactions on Power Systems*, vol. 28, no. 4, pp. 4588-4597, Nov. 2013.

Digital Object Identifier: [10.1109/TPWRS.2013.2272494](https://doi.org/10.1109/TPWRS.2013.2272494)

URL:

<http://ieeexplore.ieee.org/xpl/articleDetails.jsp?arnumber=6583292>

© 2013 IEEE. Personal use of this material is permitted. Permission from IEEE must be obtained for all other users, including reprinting/ republishing this material for advertising or promotional purposes, creating new collective works for resale or redistribution to servers or lists, or reuse of any copyrighted components of this work in other works.

Analysis of Power Sharing and Voltage Deviations in Droop-controlled DC Grids

Jef Beerten, *Member, IEEE*, and Ronnie Belmans, *Fellow, IEEE*

Abstract—This paper analyzes the influence of the converter droop settings and the DC grid network topology on the power sharing in a DC grid based on Voltage Source Converter High Voltage Direct Current (VSC HVDC) technology. The paper presents an analytical tool to study the effect of the droop control settings on the steady-state voltage deviations and power sharing after a converter outage, thereby accounting for DC grid behavior. Furthermore, an optimization algorithm is developed, taking into account two conflicting optimization criteria. The simulation results show that when selecting appropriate values for the converter gains, a trade-off has to be made between the power sharing and the maximum allowable DC voltage deviation after an outage.

Index Terms—HVDC transmission, HVDC converters, VSC HVDC, DC Grid, Voltage Droop.

I. INTRODUCTION

DUE to the large predicted increase of renewable energy sources in the power system, a significant interest has risen in DC grids based on Voltage Source Converter High Voltage Direct Current (VSC HVDC) technology. Such DC grids could e.g. be gradually developed as extensions or fundamental grid updates to interconnect remote offshore wind farms and regions with different production and consumption patterns [1], [2].

Similar to AC systems, the DC grid will have to cope with severe contingencies such as converter outages. In order to obtain a distributed system response after such events, most control schemes presented in the literature rely on DC voltage droop control, introduced in [3], [4] and extensively reported in the literature [5]–[15]. In a droop-controlled scheme, different converter jointly alleviate the power deficit caused by a converter outage, similar to the frequency control in AC systems. However, contrary to the frequency in AC systems, the DC system voltage is no global measure since the voltage varies at different DC buses as a result of the power flows in the grid.

In steady-state, the power flows can be optimized by altering the droop setpoints [9], using an Optimal Power Flow (OPF) formulation [16]. The power sharing amongst different droop-controlled converters after a contingency in the grid can be influenced by changing the converter droop constants, which determine the relation between the resulting power or current

change and the voltage deviation. Different approaches have been suggested to optimize these droop settings. In [10], the converter droop constants were calculated taking into account the DC system line resistances for a radial DC system. The procedure is however not directly applicable for meshed DC systems. In [11], the effect of the DC network on the power sharing has been studied for a meshed system. In [17], a procedure was presented to compute the droop gains ensuring stability. However, all droop coefficients were taken equal and the power sharing was not considered. In [12], the entire subset of converter droop constants was scaled to obtain optimized control settings from the point of view of the DC system dynamics. It has been implicitly assumed in the aforementioned article that the power distribution entirely depends on the relative values of the gains. In [18], it was shown that the droop settings can be optimized with respect to the power distribution in the AC system after an outage. The analysis is mainly focusing on the AC system dynamics and does not take the DC system into account. In [13], the droop coefficients were made adaptive to account for the available headroom of the different converters, using a common voltage feedback signal [19]. Other recent developments related to power flow control include the participation of the DC grid in the primary frequency control for asynchronous AC systems [14], [20], [21], the participation in the load-frequency control in one single area by means of a grid management system [22] and a slow control of the setpoints after a contingency to restore the pre-fault exchanges [23].

The effect of the droop settings on the post-fault voltage deviations and power sharing can be taken into account using power flow algorithms [15], [24], [25]. However, the power flow models are non-linear in nature and impede a straightforward analysis of the influence of the droop settings. The objective of this paper is twofold: First, the paper presents a new method to analytically study the effect of the droop settings and DC grid voltage deviations on the power flow control. The analytical method is different from the one presented in [11], where the analysis starts by assuming a lossless DC system. In this paper, the analytical expressions are first derived for a current-based droop control and are thereafter extended to a power-based droop control. Contrary to [11], the focus of this paper is merely on converter outages. Second, an optimization routine is presented. The main objective of the optimization is to show that, at least from a steady-state perspective, there are two conflicting optimization criteria when it comes to selecting the converter droop values. On the one hand, the objective is to eliminate the influence from the DC grid configuration

Jef Beerten is funded by a research grant from the Research Foundation – Flanders (FWO).

Jef Beerten and Ronnie Belmans are with the Department of Electrical Engineering (ESAT), Division ELECTA, University of Leuven (KU Leuven), Kasteelpark Arenberg 10, bus 2445, 3001 Leuven-Heverlee, Belgium. (e-mail: jef.beerten@esat.kuleuven.be, ronnie.belmans@esat.kuleuven.be)

by making the power sharing between different converters independent of the layout of the DC grid. On the other hand, the objective is to limit the steady-state voltage deviations after a contingency to reasonable values. It is shown that scaling the entire subset of converter gains, as suggested in [12], influences the steady-state power distribution and is only applicable within a limited range around a subset of droop values.

The remainder of the paper is organized as follows: Section II discusses the basic principles of converter power or current sharing after a contingency. Section III presents the analytical method to study the effect of the droop control settings as well as an equivalent representation to physically interpret the results. Section IV presents the droop control optimization. Finally, Section V presents the simulation results, including a discussion on the influence of the converter gains, line lengths and the accuracy of the power-based droop control analysis.

II. CONVERTER POWER/CURRENT SHARING

A. Voltage Droop Control

In a DC system, the DC voltage is one of the most crucial system parameters. Any current imbalance is directly reflected in a change of the DC voltage at all buses. In this section it is discussed how the voltage profile in the system influences the power or current sharing after an outage. A first part briefly revises power- and current-based droop characteristics.

With a local DC voltage used for droop control, the relation between the active DC power P_{dc} and the voltage U_{dc} at converter i can be written as

$$P_{dc_i} = P_{dc,0_i} - \frac{1}{k_{dc_i}}(U_{dc_i} - U_{dc,0_i}), \quad (1)$$

with $P_{dc,0_i}$ and $U_{dc,0_i}$ the DC power and voltage reference values and k_{dc_i} the converter droop constant at converter i .

Alternatively, the voltage droop control law can be expressed as a function of the DC current instead of the active power

$$I_{dc_i} = I_{dc,0_i} - \frac{1}{k_{dc_i}}(U_{dc_i} - U_{dc,0_i}), \quad (2)$$

with I_{dc_i} and $I_{dc,0_i}$ respectively the actual and reference DC current at converter i .

As an alternative, a common voltage feedback signal can be used as proposed in [19] and used in [13]. The droop control law then simplifies to

$$P_{dc_i} = P_{dc,0_i} - \frac{1}{k_{dc_i}}(U_{dc}^+ - U_{dc,0}^+), \quad (3)$$

with U_{dc}^+ the common converter feedback signal and $U_{dc,0}^+$ its reference value. A similar expression holds for a current-based droop control. U_{dc}^+ can be the voltage at one of the converter buses or a combination thereof. Using a common voltage feedback signal removes the voltage dependence of the power sharing after an outage. A disadvantage compared to a local voltage based droop control, is the need for communication.

B. Converter Outage

The power sharing after a converter outage can be written in terms of the voltage droop constants in the different converters. Using a current-based droop as in (2), an outage of converter i with a steady-state power injection of $I_{dc,0_i}$ gives rise to the current redistribution in the converters which can be described as

$$\Delta I_{dc_i} = -I_{dc,0_i}, \quad (4)$$

$$\Delta I_{dc_j} = I_{dc,0_i} \cdot g'_j, \quad (5)$$

where g'_j is the modified gain for converter j

$$g'_j = \frac{g_j \Delta U_{dc_j}}{\sum_{\substack{k=1 \\ k \neq i}}^m g_k \Delta U_{dc_k}}, \quad (6)$$

with $\Delta U_{dc_j} = (U_{dc_j} - U_{dc,0_j})$ and the converter gain g_j at converter j defined as the inverse of the DC droop constant k_{dc_j} . Both terms will be used interchangeably in the remainder of this paper. It can be observed from these equations that the actual redistribution of the current depends on the DC grid voltage profile after the fault, which impedes a straightforward analysis.

In case of a common voltage feedback signal used by all converters, as in (3), the relative power g'_j of converter j after a contingency can be written as

$$g'_j = \frac{g_j}{\sum_{\substack{k=1 \\ k \neq i}}^m g_k}, \quad (7)$$

thereby no longer depending on the system state after the contingency. In case of a local voltage feedback, the link between droop settings and power sharing is less apparent because of the influence of the DC voltages. When using a power-based droop as in (1), the power sharing can only approximately be written in a form similar to (4) – (5), since the DC system losses are not constant.

In the subsequent sections, the influence of the DC system voltages on the power/current sharing are discussed in detail.

III. EFFECT OF DROOP CONTROL ON THE POWER SHARING

This section presents a mathematical model to include the effect of the voltage droop control in the DC network equations. The presented method allows to easily investigate the effect of the droop settings on the power/current sharing after a converter outage.

A. Current-Based Droop Control

The DC system equations can be written in a matrix form as

$$Y_{dc} U_{dc} = I_{dc}, \quad (8)$$

with U_{dc} the DC bus voltage vector, I_{dc} containing the currents flowing into the DC system and Y_{dc} the DC system admittance matrix.

Rewriting the voltage and current vectors as

$$\mathbf{U}_{dc} = \mathbf{U}_{dc,0} + \Delta\mathbf{U}_{dc}, \quad (9)$$

$$\mathbf{I}_{dc} = \mathbf{I}_{dc,0} + \Delta\mathbf{I}_{dc}, \quad (10)$$

the DC system equations can be rewritten as

$$\mathbf{Y}_{dc}\Delta\mathbf{U}_{dc} - \Delta\mathbf{I}_{dc} = \mathbf{I}_{dc,0} - \mathbf{Y}_{dc}\mathbf{U}_{dc,0}. \quad (11)$$

For the current-based droop control from (2),

$$\Delta\mathbf{I}_{dc} = -\mathbf{G}\Delta\mathbf{U}_{dc}, \quad (12)$$

with $\mathbf{G} = \text{diag}([g_1 \cdots g_n])$ a diagonal matrix comprised of the converter gains g_i , which are given by the inverse droop coefficients, i.e. $k_{dc_i}^{-1}$ from (2). Replacing the voltage and current references $\mathbf{U}_{dc,0}$ and $\mathbf{I}_{dc,0}$ with the values corresponding to the situation before the converter outage, which satisfy (8), and substituting (12), the DC system equations simplify to

$$(\mathbf{Y}_{dc} + \mathbf{G})\Delta\mathbf{U}_{dc} = 0, \quad (13)$$

with the trivial solution $\Delta\mathbf{U}_{dc} = 0$ as the only solution provided that $\det(\mathbf{Y}_{dc} + \mathbf{G}) \neq 0$.

A converter under constant current control or a DC bus without a converter, hence without current injection, can be represented by altering matrix \mathbf{G} such that

$$\mathbf{G} = \begin{bmatrix} 0 & & & \\ & g_2 & & \\ & & \ddots & \\ & & & g_n \end{bmatrix}, \quad (14)$$

assuming the first bus to have a constant current injection (or zero converter gain). In case of a DC bus without injection, the current injection vector $\mathbf{I}_{dc,0}$ has to be updated accordingly.

Similarly, the effect of an outage of converter i on the voltages can be addressed by defining a modified gain matrix

$$\mathbf{G}_{\text{out}} = \text{diag}([g_1 \cdots g_{i-1} \ 0 \ g_{i+1} \cdots g_n]). \quad (15)$$

As in the previous case, a zero entry can be added to $\mathbf{I}_{dc,0}$ in (11), or alternatively, applying the superposition principle, the voltage deviations after the outage can be found by solving

$$(\mathbf{Y}_{dc} + \mathbf{G}_{\text{out}})\Delta\mathbf{U}_{dc} = \mathbf{I}_{dc,\text{out}}, \quad (16)$$

with the current outage vector $\mathbf{I}_{dc,\text{out}}$ defined as $\mathbf{I}_{dc,\text{out}} = [0 \cdots 0 \ -I_{dc,0_i} \ 0 \cdots 0]^T$. The matrix \mathbf{G}_{out} expresses the effect of the voltage change on the currents injected by the droop-controlled converters.

The change of the converter current injections can thereafter be determined by calculating $\Delta\mathbf{I}_{dc}$ from

$$\Delta\mathbf{I}_{dc} = \mathbf{Y}_{dc}\Delta\mathbf{U}_{dc} = -\mathbf{G}_{\text{out}}\Delta\mathbf{U}_{dc}. \quad (17)$$

It is clear from (6) that similar voltage deviations give rise to a current sharing that approximates the case of a common voltage feedback in (7). As discussed in the remainder of the paper, it can be shown that decreasing line resistances or decreasing the converter gains g_i lead to a more uniform voltage deviation profile in the network.

In case of a slack converter (constant DC voltage), the steady-state value of the DC voltage is constant. Hence, the

corresponding row and column can be removed from (16). In case of more advanced droop control schemes (e.g. with a current/voltage deadband), the droop characteristics can be considered to be a combination of a basic droop characteristic and a constant current or voltage part.

B. Power-Based Droop Control

In case of a power-based droop control as in (1) or a constant power control, the analysis is somewhat complicated due to the fact that the power flow equations become nonlinear. It is either possible to solve the full set of power flow equations as in [24] or to use an approach similar to the one from the previous part.

The power-based droop from (1) can be rewritten as

$$I_{dc_i} = \frac{P_{dc_i}}{p U_{dc_i}} = \frac{P_{dc,0_i}}{p U_{dc_i}} - \frac{1}{p k_{dc_i}} \left(1 - \frac{U_{dc,0_i}}{U_{dc_i}}\right), \quad (18)$$

with $p = 1$ for an asymmetrical monopolar grid and $p = 2$ for a symmetrical monopolar or bipolar grid. A similar expression holds for a constant power converter

$$I_{dc_i} = \frac{P_{dc_0}}{p U_{dc_i}}. \quad (19)$$

With U_{dc} as defined in (9), I_{dc} can be approximated by the Taylor series expansion about $U_{dc,0}$. For (18) and (19), this respectively results in

$$I_{dc_i} \approx I_{dc,0_i} - \frac{1}{U_{dc,0_i}} \left(\frac{1}{p k_{dc_i}} + I_{dc,0}\right) \Delta U_{dc_i}, \quad (20)$$

$$I_{dc_i} \approx I_{dc,0_i} - \frac{I_{dc,0_i}}{U_{dc,0_i}} \Delta U_{dc_i}. \quad (21)$$

Defining modified gains g_i^* with

$$g_i^* = \frac{1}{p k_{dc_i} U_{dc,0_i}} + \frac{I_{dc,0_i}}{U_{dc,0_i}}, \quad (22)$$

and using the superposition principle, the DC system equations (11) can be rewritten such that

$$(\mathbf{Y}_{dc} + \mathbf{G}^* + \mathbf{L})\Delta\mathbf{U}_{dc} = 0, \quad (23)$$

with \mathbf{G}^* and \mathbf{L} diagonal matrices with either $G_{jj}^* = g_j^*$ or $L_{jj} = I_{dc,0_j}/U_{dc,0_j}$, depending on whether bus j is modeled as a power-based droop or constant power bus. In case of a converter outage, the same analysis can be applied, retaining

$$(\mathbf{Y}_{dc} + \mathbf{G}_{\text{out}}^* + \mathbf{L}_{\text{out}})\Delta\mathbf{U}_{dc} = \mathbf{I}_{dc,\text{out}}, \quad (24)$$

with the outage matrices $\mathbf{G}_{\text{out}}^*$ and \mathbf{L}_{out} defined similar to (15), with the matrix elements $G_{\text{out}_{ii}}^*$ or $L_{\text{out}_{ii}}$ equal to zero for an outage of converter i . The matrices $\mathbf{G}_{\text{out}}^*$ and \mathbf{L}_{out} express the effect of the voltage change on the current injected by respectively the power droop-controlled and constant power buses not facing an outage. Using this first-order approximation, the power distribution can thereafter be expressed as

$$\Delta P_{dc} \approx p \cdot (\mathbf{U}_{dc,0} + \Delta\mathbf{U}_{dc}) \circ (\mathbf{I}_{dc,0} + \Delta\mathbf{I}_{dc}) - P_{dc,0}, \quad (25)$$

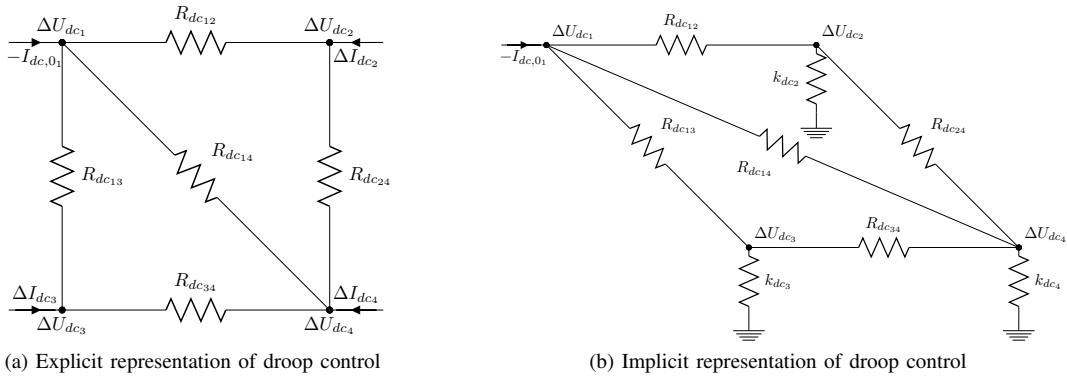


Fig. 1. Electrical equivalent scheme of a DC grid with current-based voltage droop control.

with \circ the Hadamard or entrywise product. Alternatively, the power distributed amongst the slack buses can also be approximated as

$$\Delta P_{dc} \approx -G_{out} \Delta U_{dc}, \quad (26)$$

with G_{out} as defined in (15). It was found that (25) leads to more accurate results than (26). Similar to the previous section, a constant voltage bus can be represented by omitting the corresponding equation in (24). Advanced droop schemes can here as well be analyzed by modeling the converters as a combination of the respective representations.

C. Equivalent Electrical Model

The inclusion of the droop-controlled (and constant power) buses can be regarded as a change of the DC network admittance matrix, hence we define a modified admittance matrix

$$Y'_{dc} = Y_{dc} + G_{out}, \quad (27)$$

in case of a current-based droop and

$$Y'_{dc} = Y_{dc} + G_{out}^* + L_{out}, \quad (28)$$

in case of a power-based droop.

Mathematically, the converter gains and contributions from constant power buses are added to the diagonal of the network admittance matrix. From an electric point of view, these changes to the admittance matrix can be interpreted as the inclusion of shunt loads to the respective buses in the DC network, as depicted in Fig. 1.

With an outage of converter 1, the system of equations can be partitioned such that

$$\begin{bmatrix} Y'_{dc_{11}} & Y'_{dc_{1\alpha}} \\ Y'_{dc_{\alpha 1}} & Y'_{dc_{\alpha\alpha}} \end{bmatrix} \begin{bmatrix} \Delta U_{dc_1} \\ \Delta U_{dc_\alpha} \end{bmatrix} = \begin{bmatrix} -I_{dc,0_1} \\ \mathbf{0} \end{bmatrix}, \quad (29)$$

with ΔU_{dc_α} containing the voltages of the buses without an outage. Using the Kron reduction technique, discussed in greater detail in [26], the nodes without current injections can be considered as internal nodes that can be eliminated. These are all the nodes but the one facing an outage, as can be seen from Fig. 1b. The network can thus be reduced and the voltage change at the bus facing an outage can be rewritten as

$$\Delta U_{dc_1} = - \left(Y'_{dc_{11}} - Y'_{dc_{1\alpha}} Y'_{dc_{\alpha\alpha}}^{-1} Y'_{dc_{\alpha 1}} \right)^{-1} I_{dc,0_1}. \quad (30)$$

This equation expresses the relationship between the current injection change due to an outage and the resulting voltage change at that bus, taking into account the droop control actions. It can be observed that the corresponding resistance value from (30) corresponds to element $Z'_{dc_{11}}$ from the modified DC bus impedance matrix Z'_{dc} . Therefore, the voltage change at the internal (droop-controlled) buses can be equally found by rewriting (16) in terms of this modified impedance matrix Z'_{dc} such that

$$\Delta U_{dc_\alpha} = -Z'_{dc_{\alpha 1}} I_{dc,0_1}, \quad (31)$$

using a partitioning similar to (29).

It is clear from this representation that when the gains $g_i = k_{dc_i}^{-1}$ decrease, the equivalent loads are reduced and the resulting network from Fig. 1b approximates the original DC network. As a result, the condition number $\kappa(Y'_{dc})$ increases and in the limiting case of the set of gains g_i going to zero (and hence the droop constants k_{dc_i} going to infinity), Y'_{dc} becomes singular. From a physical point of view, a set of converters with lower gains (or high droop constants) result in higher voltage deviations ΔU_{dc} after an outage. Since a decreased set of gains has a lower influence on Y'_{dc} in (27), the voltage profile gets more uniform and it becomes easier to influence the current distribution after an outage by choosing the relative values of the converter gains. On the contrary, if the converter gains g_i go to infinity the equivalent loads from Fig. 1b increase and the voltage deviations ΔU_{dc} go to zero. Due to the resulting dominance of G_{out} in the modified admittance matrix Y'_{dc} from (27), the voltage deviations become less uniformly distributed in relative terms and the different converters have a tendency to share a power or current deficit in a non-uniform manner.

A similar reasoning holds for power-based droop control. As can be observed from (13) – (16) and (23) – (24) the modified converter gains g_j^* from (22) are added to the diagonal of the network admittance matrix. Also in case of constant power controlled buses, diagonal elements derived in (21) are added to take into account the effect of a voltage change on the current injections, following a similar reasoning as with current-based droop controllers. However, one has to keep in mind that in this case the equations are linearized, whereas they exactly hold in case of a current-based droop control.

IV. MULTIOBJECTIVE DROOP CONTROL OPTIMIZATION

The optimization routine presented in this paper shows that there are two conflicting optimization criteria when it comes to setting the converter gains or droop values. On the one hand, the objective is to eliminate the influence from the DC grid configuration by making the power or current sharing between different converters independent of the layout of the DC grid. On the other hand, the objective is to limit the steady-state voltage deviations to reasonable values. The analysis in this section uses a current-based droop control. In Section V, the accuracy of the power-based droop control analysis is discussed, providing an indication of the applicability of the optimization algorithm for the power-based variant.

The first objective is to limit the voltage deviations after an outage for an arbitrary converter, hence

$$f_1(\mathbf{x}) = \sum_{i=1}^n \xi_i \sum_{j=1}^n (\Delta U_{dc_j}^i)^2, \quad (32)$$

with $\Delta U_{dc_j}^i$ the voltage deviation at converter j after an outage of converter i , ξ_i a weighting factor accounting for the probability or the relative importance of an outage of converter i , and the optimization vector \mathbf{x}

$$\mathbf{x} = \left[\mathbf{g}^T \ \Delta \mathbf{U}_{dc}^1{}^T \ \cdots \ \Delta \mathbf{U}_{dc}^n{}^T \right]^T, \quad (33)$$

with \mathbf{g} the set of converter gains and $\Delta \mathbf{U}_{dc}^i$ a vector containing the set of voltage deviations after an outage of converter i .

The second objective is to limit the deviation from a predefined current distribution after any outage or

$$f_2(\mathbf{x}) = \sum_{i=1}^n \xi_i \sum_{j=1}^n (g_j \Delta U_{dc_j}^i - \Delta I_{dc_j}^{*i})^2, \quad (34)$$

with $\Delta I_{dc_j}^{*i}$ the setpoint of the change in current injection at converter j for an outage of converter i . Optimizing towards an equal distribution of the current between the remaining $n-1$ converters results in

$$\Delta I_{dc_j}^{*i} = \frac{I_{dc_i}}{n-1}. \quad (35)$$

Similarly, it is possible to optimize towards an unequal current distribution by introducing a distribution priority variable ζ for each converter such that

$$\Delta I_{dc_j}^{*i} = \frac{\zeta_j}{\sum_{\substack{k=1 \\ k \neq i}}^n \zeta_k} I_{dc_i}, \quad (36)$$

thereby neglecting the influence of the DC grid when defining the optimal current sharing.

If converters already operate close to their limits, this can implicitly be accounted for by an appropriate selection of the distribution priority variables ζ . Alternatively, the limits can explicitly be defined by including additional inequality constraints for the converter current or power.

The voltage deviations have to satisfy (16) with \mathbf{Y}'_{dc} from (27) or

$$\mathbf{h}^i(\mathbf{x}) = \mathbf{Y}'_{dc}(\mathbf{g}) \Delta \mathbf{U}_{dc}^i - \mathbf{I}_{dc,out}^i \quad 1 \leq i \leq n. \quad (37)$$

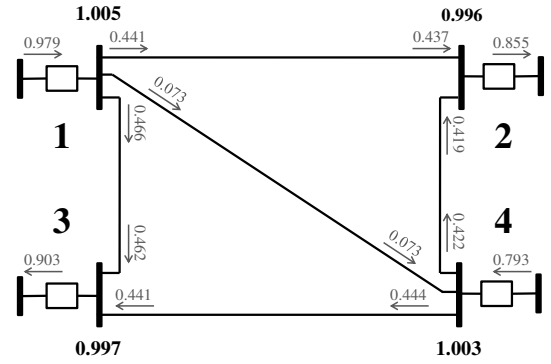


Fig. 2. Test-system – Power flow situation before the outage.

TABLE I
DC GRID LINE RESISTANCES AND LENGTHS

line	$R_{dc_{ij}}$ (p.u.)	length l (km)
1 – 2	0.0411	290
1 – 3	0.0356	251
1 – 4	0.0463	327
2 – 4	0.0349	246
3 – 4	0.0297	209

The optimization problem can be written by combining the two objective functions using a weighting factor $w \in [0, 1]$

$$\text{minimize } f(\mathbf{x}) = (1-w)f_1(\mathbf{x}) + wf_2(\mathbf{x}), \quad (38)$$

$$\text{subject to } \mathbf{h}^i(\mathbf{x}) \quad 1 \leq i \leq n. \quad (39)$$

In the case of a power-based droop control or constant power buses, the modified admittance matrix \mathbf{Y}'_{dc} from (37) is replaced with the definition from (28). This yields a linearization of the power flow equations and hence of the constraints in (37). The validity of using this linearization is addressed in the last part of the next section.

V. SIMULATION RESULTS

The proposed optimization method has been implemented with a ± 320 kV 4-terminal DC grid test system shown in Fig. 2. All converters have a rated output of 1200 MW. The per unit line resistances are given in Table I with the unit base quantities $P_{dc,b} = 1200$ MW, $U_{dc,b} = 320$ kV and $I_{dc,b} = P_{dc,b}/U_{dc,b}$. The sum of the system admittance matrix \mathbf{Y}_{dc} and the converter gain matrix \mathbf{G} is given by

$$\begin{bmatrix} 74.019 + g_1 & -24.331 & -28.090 & -21.598 \\ -24.331 & 52.984 + g_2 & 0 & -28.653 \\ -28.090 & 0 & 61.760 + g_3 & -33.670 \\ -21.598 & -28.653 & -33.670 & 83.922 + g_4 \end{bmatrix}. \quad (40)$$

A. Multiobjective Droop Control Optimization

All possible converter outages are considered equally important in the optimization ($\xi_i = 1$). The analysis is limited to the current-based droop control, but a similar approach can be used for the power-based droop control. Section V-D discusses the accuracy of the power-based droop approximation from Section III-B.

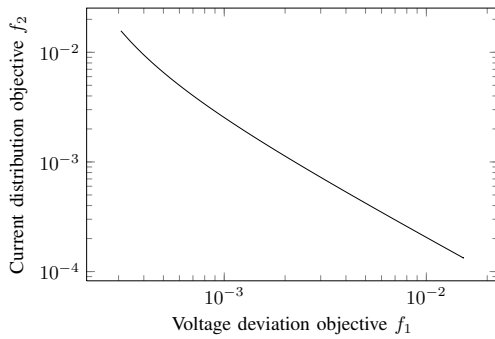


Fig. 3. Pareto-optimal trade-off curve between the objective of minimizing the voltage deviations (f_1) and the objective of equalizing the current distribution (f_2) for all possible converter outages.

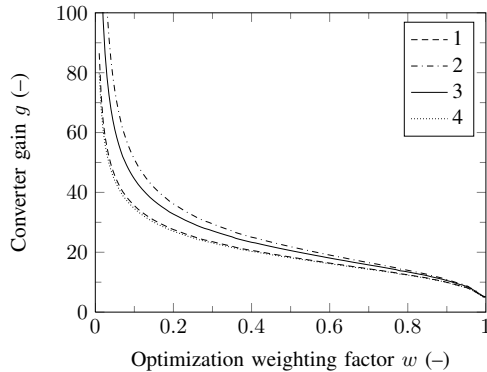


Fig. 4. Converter gains g as a function of the optimization weighting factor w .

Unlike the first optimization objective (32), which is quadratic, the second optimization objective (34) is non-linear. This holds as well for the equality constraints (37) due to the dependence of matrix Y'_{dc} on the unknown set of gains g . Since the overall problem is non-linear, it is solved using the generic non-linear optimization routine `fmincon` from the Optimization Toolbox in MATLAB. The multiobjective optimization problem (38) – (39) is sequentially solved for different values of the weighting factor w .

Fig. 3 shows the Pareto-optimal trade-off curve between the two objective functions f_1 and f_2 . It can be observed that a trade-off is indeed present between equalizing the current distribution (objective f_2) on the one hand and limiting the DC voltage deviations (objective f_1) on the other hand.

Fig. 4 shows the converter gains g as a function of the optimization weighting factor w defined in (38). The graph shows that the converter gains decrease when more emphasis is put on the current distribution after an outage (high value of w) and that the gains increase if the voltage deviation has to be limited.

Figs. 5 – 6 show the voltage deviations and the current distribution after an outage of converter 2 as a function of the optimization weighting factor w . Comparing the results with Fig. 4, it can be observed that the voltage deviations increase with decreasing converter gains and vice versa. Furthermore, Fig. 6 indicates that it can be practically impossible to get an equal current contribution for all converter outages at the same

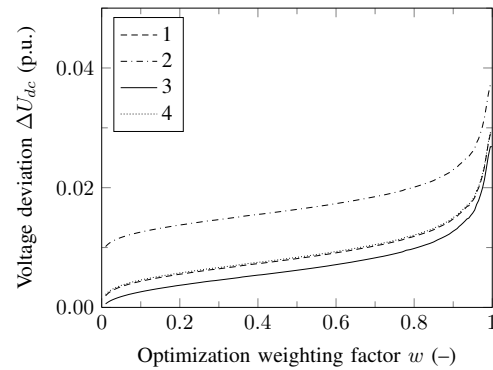


Fig. 5. Outage of converter 2 – Voltage deviations ΔU_{dc} as a function of the optimization weighting factor w .

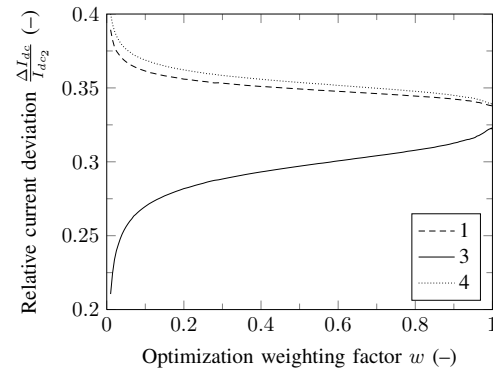


Fig. 6. Outage of converter 2 – Relative current sharing $\Delta I_{dc}/I_{dc2}$ as a function of the optimization weighting factor w .

time. It can be observed that converters 1 and 4 take a higher share of the current deficit, since they are located closer to converter 2 facing an outage. Comparing Fig. 4 with Table I, it can be observed that the network topology is accounted for by the optimization algorithm as the gains for converters 2 and 3 are slightly higher, since these converters only have two connections instead of 3.

B. Influence of the Converter Gain

Figs. 7 – 9 show the results from Figs. 4 – 6, now as a function of the gain g_1 of converter 1. From the voltage deviations in Fig. 7 it is clear that for small gain values g (and thus high droop constants k_{dc}), the voltage deviations inversely depend on the gain values and approximately linearly depend on the droop constants. When the gain increases and the droop values k_{dc} become of the order of magnitude of the line resistances (Table I), this approximation comes to an end.

From Fig. 8, it is clear that an equal current distribution is only feasible when the gain values are chosen very low. This relative current distribution from Fig. 8 is a result of the optimization and therefore takes into account all possible converter outages. Fig. 9 shows how the relative gain values increase as a function of the increasing gain at converter 1. With an increasing gain, a higher emphasis is put on f_1 , i.e. the voltage deviation minimization, whilst still minimizing f_2 and hence striving towards an equal current distribution. In [12], the set of gain values was optimized from the point of

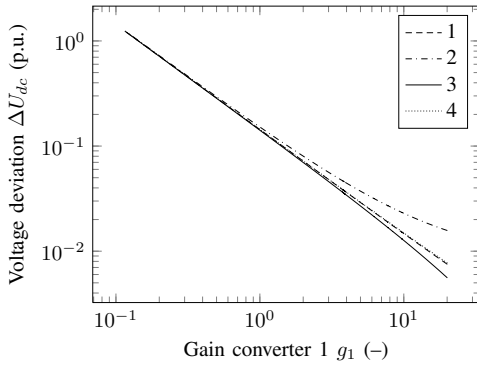


Fig. 7. Outage of converter 2 – Voltage deviations ΔU_{dc} as a function of the gain of converter 1.

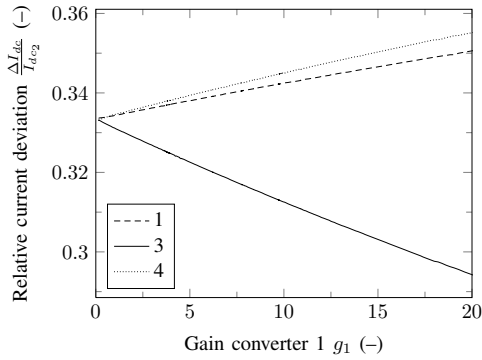


Fig. 8. Outage of converter 2 – Relative current sharing $\Delta I_{dc}/I_{dc2}$ as a function of the gain of converter 1.

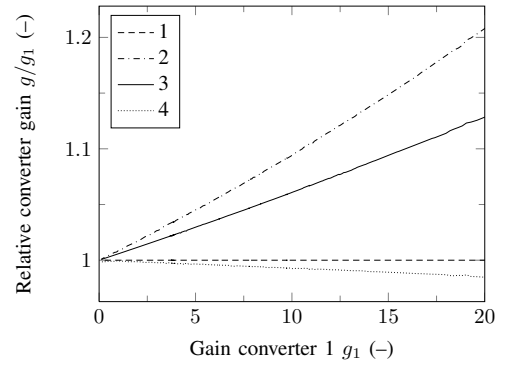


Fig. 9. Outage of converter 2 – Relative converter gains g/g_1 as a function of the gain of converter 1.

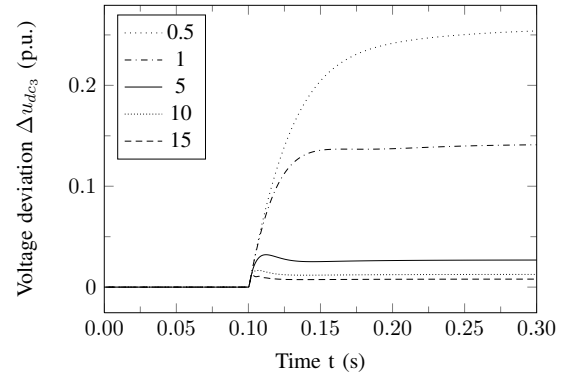


Fig. 10. Outage of converter 2 – Voltage deviation Δu_{dc3} at converter 3 for different values of the gain of converter 1 (Time simulations).

view of the DC system dynamics. It was argued that this set of relative gain values could be scaled, resulting in a similar current distribution. From Figs. 8 – 9, it can be seen that when the average gain value is increased, the relative gain settings change and the current becomes less equally distributed, even when still taking an equal distribution as an optimization criteria. Fig. 9 shows that the gain of converter 2 changes more slowly than that of converter 1, which is explained by the fact that the line distances to converter 4 are slightly lower than the ones to bus 1 (Table I). An opposite reasoning holds for the relatively higher increase of the converter gains in 2 and 3. However, an opposite trend is observed for the current distributions in Fig. 8. It is clear that, although having a relatively higher gain value in converter 3 than in converter 1, the part of the current deficit accounted for by converter 3 decreases, whereas it increases more for converter 4, although having a relatively lower gain than converter 1. According to the current sharing expressions from (4) – (6), this means that the increase in converter gain is not high enough to account for the (unequally) decreasing voltage deviations ΔU_{dc} . This also implies that scaling all gains using fixed ratios, as suggested in [12], leads to a change of the current distribution, that would be even more unequal in this example.

Figs. 10 – 11 show corresponding time domain responses of the DC current and voltage at converter 3 for a selected number of gain settings. The current-based droop control has been implemented using an averaged converter model in *MatDyn*,

an open-source MATLAB-based stability program [27]. The values indicated in Figs. 10 – 11 refer to the gain of converter 1. The absolute gain values of the other converters are found using the corresponding relative values from Fig. 9. The DC network has been represented by lumped π -equivalent models including line resistance, cable and converter capacitance.

As is clear from Figs. 10 – 11, the permissible values of the converter gains are limited: On the one hand, the dynamic response of the DC system puts an upper limit to the gain values, as discussed in [12]. On the other hand, the gains cannot be chosen too low to avoid that the voltages deviate too much from their setpoints.

C. Influence of the Line Length

In [11], it was shown that, when keeping the gains constant, an increasing transmission line distance to one particular bus results in a decreasing power balance from that particular bus. With similar gain values at different converters, a DC grid therefore has the tendency to solve imbalances locally.

These findings are confirmed in this paper when accounting for the line lengths in the optimization. This has been analyzed by scaling the lines to bus 3 by a scale factor γ . The optimization has been repeated for a fixed value of $w = 0.9924$, which corresponds to gain values of about 5 for $\gamma = 1$. Figs. 12 – 13 respectively show the voltage deviations after an outage of converter 2 and the converter gains as a function of the scale factor γ . Fig. 13 demonstrates that, when bus 3 is more remote

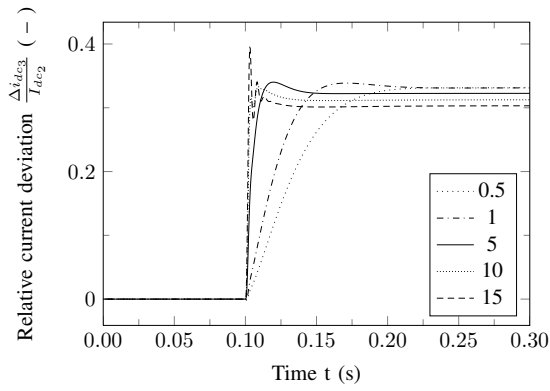


Fig. 11. Outage of converter 2 – Relative current sharing $\Delta i_{dc3}/I_{dc2}$ at converter 3 for different values of the gain of converter 1 (Time simulations).

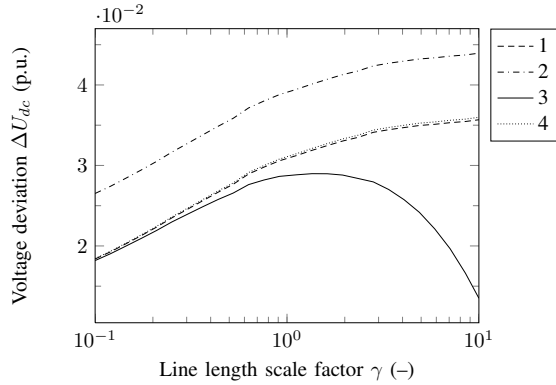


Fig. 12. Outage of converter 2 – Voltage deviations ΔU_{dc} as a function of the line length scaling factor γ (Scaling of lines 1 – 3 and 3 – 4).

(large values of scale factor γ), the converter gain at bus 3 g_3 has to be increased to maintain the current distribution as equally balanced as possible (objective function f_2 has been given a relatively high priority). Similarly, the voltage drop at bus 3 decreases, indicating that a remote bus as such is less affected by converter outages and requires a higher converter gain.

When the transmission line length decreases (low values of scale factor γ), the optimal gain of converter g_3 approximates that of the nearby converters 1 and 4. For the same value of the optimization weighting factor w , the converter gains can be increased since the different buses in the network become more strongly coupled, resulting in lower voltage drops.

D. Accuracy of the Power-Based Droop Control Analysis

The analysis in this paper has been limited to current-based droop converters. The results exactly hold, as all equations from Section III-A are linear. For the power-based droop controller, a similar methodology was developed in Section III-B by linearizing the system at the pre-fault working point. In this part, it is analyzed to what extent the results for the linearized power-based droop control deviate from the actual results obtained by a power flow analysis. The power flow results have been obtained using MATACDC, a free open-source power flow analysis toolbox for hybrid AC/DC systems [28], using the power flow droop formulation from [15]. The

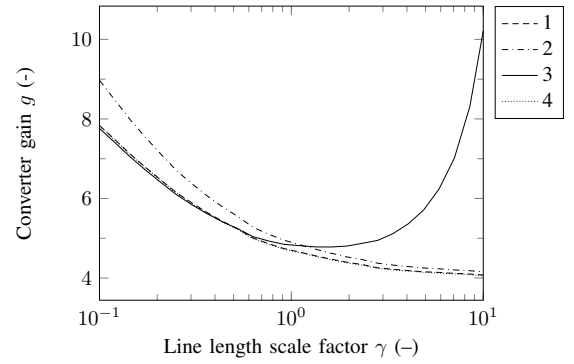


Fig. 13. Outage of converter 2 – Converter gains g as a function of the line length scaling factor γ (Scaling of lines 1 – 3 and 3 – 4).

errors of the voltage and power deviations, respectively ϵ_U and ϵ_P , are shown in Figs. 14 – 15 for an outage of converter 2. The errors ϵ_U and ϵ_P for converter i are respectively defined as

$$\epsilon_{U_i} = \frac{\Delta U_{dc_i} - \Delta U_{dc,PF_i}}{\Delta U_{dc,PF_i}}, \quad (41)$$

$$\epsilon_{P_i} = \frac{\Delta P_{dc_i} - \Delta P_{dc,PF_i}}{\Delta P_{dc,PF_i}}, \quad (42)$$

with $\Delta U_{dc,PF_i}$ and $\Delta P_{dc,PF_i}$ respectively the voltage and power deviations calculated using the power flow routines, with a tolerance of $1e-12$ for the DC system power flow. All converter gains have been chosen equal and are shown on the x -axis in Figs. 14 – 15. When compared with the results of the current-based droop control, a scaling factor of 2 has to be taken into account such that $g_P = 2g_I$, in correspondence to the per unit convention $I_{dc,b} = P_{dc,b}/U_{dc,b}$. The current-based converter gain g_I of 5 used in the previous section thus corresponds to a power-based gain g_P of 10. This gain value has been decreased and increased up to a factor 10, as shown in Figs. 14 – 15. It can be observed that linearizing the power flow equations still leads to accurate results as long as the gain values are not too low. For low gain values g (or high droop values k_{dc}), the errors increase due to the relatively higher share of the droop-independent term in (22), approximating the droop controller as a linearized constant power control.

From these results, it can be concluded that linearizing the power-based equations, as done in Section III-B, still yields good results for a wide range of droop values and can be used to estimate the system response after a contingency for realistic droop settings. However, the method cannot be used to obtain accurate results in case the gains are chosen unrealistically low. As an example, the system response with a power-based gain g_P of 10, approximately corresponding to a current-based gain g_I of 5, leads to voltage drops in the range of a few percents according to Fig. 7 and a reasonable accuracy according to Figs. 14 – 15. When the gain is decreased by a factor 10, the voltage deviation roughly increases by a factor 10 for the same outage, already yielding unrealistic high values and therefore unrealistic low gain settings.

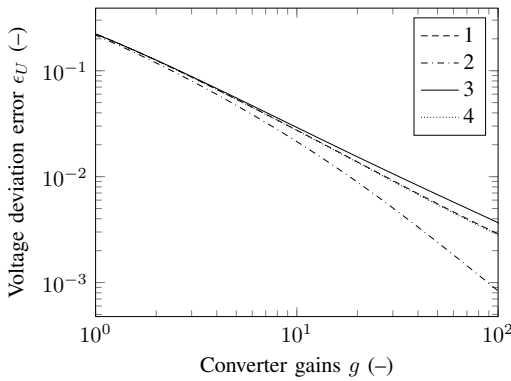


Fig. 14. Outage of converter 2 – Voltage deviation error ϵ_U as a function of the converter gains g .

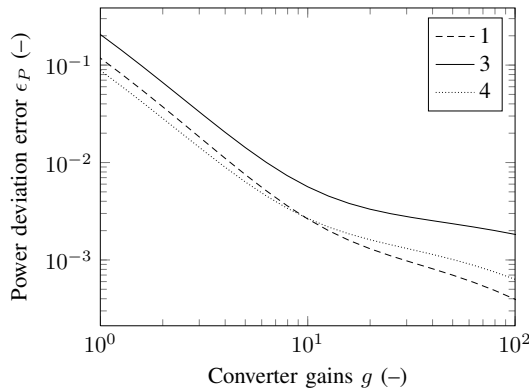


Fig. 15. Outage of converter 2 – Power deviation error ϵ_P as a function of the converter gains g .

VI. CONCLUSION

In this paper, a method has been derived to address the power and current sharing after a converter outage in a DC grid. The method can both be applied for current-based and power-based droop control, but the accuracy for the power-based droop control decreases with decreasing converter gains. An optimization routine has been presented to show the trade-off one has to make between limiting the steady-state voltage deviations after a contingency and striving for an optimal current redistribution after a converter outage. A set of gain values can therefore only be scaled to a limited extent without altering the current distribution. By varying the line lengths, it has been shown that, with comparable converter gain values, the DC grid has a tendency to solve deficits locally.

REFERENCES

- [1] D. Van Hertem and M. Ghandhari, "Multi-terminal VSC HVDC for the European supergrid: Obstacles," *Renewable and Sustainable Energy Reviews*, vol. 14, no. 9, pp. 3156–3163, Dec. 2010.
- [2] J. D. Decker and A. Woyte, "Review of the various proposals for the European offshore grid," *Renewable Energy*, vol. 49, pp. 58–62, 2013, selected papers from World Renewable Energy Congress - XI.
- [3] R. Hendriks, G. Paap, and W. Kling, "Control of a multi-terminal VSC transmission scheme for connecting offshore wind farms," in *Proc. European Wind Energy Conference & Exhibition*, Milan, Italy, May 7–10, 2007, 8 pages.
- [4] T. M. Haileselassie, M. Molinas, and T. Undeland, "Multi-terminal VSC-HVDC system for integration of offshore wind farms and green electrification of platforms in the North Sea," in *Proc. NORPIE 2008*, Espoo, Finland, Jun. 19–21, 2008, 8 pages.
- [5] C. Barker and R. Whitehouse, "Autonomous converter control in a multi-terminal HVDC system," in *Proc. IET ACDC 2010*, London, UK, Oct. 20–21, 2010, 5 pages.
- [6] W. Wang, M. Barnes, and O. Marjanovic, "Droop control modelling and analysis of multi-terminal VSC-HVDC for offshore wind farms," in *Proc. IET ACDC 2012*, Birmingham, UK, Dec. 4–6, 2012, 6 pages.
- [7] O. Gomis-Bellmunt, J. Liang, J. Ekanayake, and N. Jenkins, "Voltage-current characteristics of multiterminal HVDC-VSC for offshore wind farms," *Electric Power Systems Research*, vol. 81, pp. 440–450, 2011.
- [8] A. Egea-Alvarez, F. Bianchi, O. Gomis Bellmunt, A. Junyent-Ferre, and G. Gross, "Voltage control of multiterminal VSC-HVDC transmission systems for offshore wind power plants: Design and implementation in a scaled platform," *IEEE Trans. Ind. Electron.*, vol. 60, no. 6, pp. 2381–2391, Jun. 2012.
- [9] M. Aragüés-Peñalba, A. Egea-Álvarez, O. Gomis-Bellmunt, and A. Sumper, "Optimum voltage control for loss minimization in HVDC multi-terminal transmission systems for large offshore wind farms," *Electric Power Systems Research*, vol. 89, pp. 54–63, 2012.
- [10] L. Xu, L. Yao, and M. Bazargan, "DC grid management of a multi-terminal HVDC transmission system for large offshore wind farms," in *Proc. SUPERGEN '09*, 2009, 7 pages.
- [11] T. M. Haileselassie and K. Uhlen, "Impact of DC line voltage drops on power flow of MTDC using droop control," *IEEE Trans. Power Syst.*, vol. 27, no. 3, pp. 1441–1449, Aug. 2012.
- [12] E. Prieto-Araujo, F. D. Bianchi, A. Junyent-Ferre, and O. Gomis-Bellmunt, "Methodology for droop control dynamic analysis of multiterminal VSC-HVDC grids for offshore wind farms," *IEEE Trans. Power Del.*, vol. 26, no. 4, pp. 2476–2485, 2011.
- [13] N. R. Chaudhuri and B. Chaudhuri, "Adaptive droop control for effective power sharing in multi-terminal DC (MTDC) grids," *IEEE Trans. Power Syst.*, vol. 28, no. 1, pp. 21–29, Feb. 2013.
- [14] T. Haileselassie and K. Uhlen, "Primary frequency control of remote grids connected by multi-terminal HVDC," in *Proc. IEEE PES GM 2010*, Minneapolis, USA, Jul. 25–29, 2010, 6 pages.
- [15] J. Beerten, D. Van Hertem, and R. Belmans, "VSC MTDC systems with a distributed DC voltage control – a power flow approach," in *Proc. IEEE PowerTech '11*, Trondheim, Norway, Jun. 19–23, 2011, 6 pages.
- [16] R. Wiget and G. Andersson, "Optimal power flow for combined AC and multi-terminal HVDC grids based on VSC converters," in *Proc. IEEE PES GM 2012*, San Diego, USA, Jul. 22–26, 2012, 8 pages.
- [17] F. Bianchi and O. Gomis-Bellmunt, "Droop control design for multi-terminal VSC-HVDC grids based on LMI optimization," in *Proc. IEEE CDC-ECC 2011*, Florida, USA, Dec. 12–15, 2011, pp. 4823–4828.
- [18] J. Beerten, R. Eriksson, and R. Belmans, "Influence of DC voltage droop settings on AC system stability," in *Proc. IET ACDC 2012*, Birmingham, UK, Dec. 4–6, 2012, 6 pages.
- [19] B. Berggren, R. Majumder, C. Sao, and K. Lindén, "Method and control device for controlling power flow within a dc power transmission network," Patent WIPO International Publication Number WO 2012/000 549A1, International Filing Date: Jun. 30, 2010.
- [20] A. Sarlette, J. Dai, Y. Phulpin, and D. Ernst, "Cooperative frequency control with a multi-terminal high-voltage DC network," *Automatica*, vol. 48, no. 12, pp. 3128–3134, 2012.
- [21] N. R. Chaudhuri, R. Majumder, and B. Chaudhuri, "System frequency support through multi-terminal DC (MTDC) grids," *IEEE Trans. Power Syst.*, vol. 28, no. 1, pp. 347–356, Feb. 2013.
- [22] A.-K. Marten and D. Westermann, "Power flow participation by an embedded HVDC grid in an interconnected power system," in *Proc. IEEE ISGT Europe 2012*, Berlin, Germany, Oct. 14–17, 2012, 6 pages.
- [23] A. Egea-Alvarez, J. Beerten, D. Van Hertem, and O. Gomis-Bellmunt, "Primary and secondary power control of multiterminal HVDC grids," in *Proc. IET ACDC 2012*, Birmingham, UK, Dec. 4–6, 2012, 6 pages.
- [24] J. Beerten, S. Cole, and R. Belmans, "Generalized steady-state VSC MTDC model for sequential AC/DC power flow algorithms," *IEEE Trans. Power Syst.*, vol. 27, no. 2, pp. 821–829, May 2012.
- [25] M. Baradar and M. Ghandhari, "A multi-option unified power flow approach for hybrid AC/DC grids incorporating multi-terminal VSC-HVDC," *IEEE Trans. Power Syst.*, 2013, accepted for publication.
- [26] F. Dörfler and F. Bullo, "Kron reduction of graphs with applications to electrical networks," *IEEE Trans. Circuits Syst. I*, vol. 60, no. 1, pp. 150–163, Jan. 2013.

- [27] S. Cole and R. Belmans, "MatDyn, a new Matlab-based toolbox for power system dynamic simulation," *IEEE Trans. Power Syst.*, vol. 26, no. 3, pp. 1129–1136, 2011.
- [28] MatACDC website. [Online]. Available: <http://www.esat.kuleuven.be/electa/teaching/matacdc/>



Jef Beerten (S'07-M'13) was born in Belgium in 1985. He received the M.Sc. degree in electrical engineering from the University of Leuven (KU Leuven), Leuven, Belgium, in 2008, and the Ph.D. degree in 2013, also from KU Leuven. He is a Postdoctoral Researcher with the ESAT-ELECTA division of KU Leuven. His research interests include power system control, the grid of the future and multiterminal VSC HVDC in particular. Mr. Beerten is an active member of both the IEEE and CIGRÉ.

Mr. Beerten's research has been funded by a Ph.D. fellowship from the Research Foundation – Flanders (FWO). Currently, he holds a postdoctoral fellowship from the FWO.



Ronnie Belmans (S'77-M'84-SM'89-F'05) received the M.Sc. degree in electrical engineering in 1979 and the Ph.D. degree in 1984, both from the University of Leuven (KU Leuven), Belgium, the Special Doctorate in 1989 and the Habilitation in 1993, both from the RWTH, Aachen, Germany. Currently, he is a full professor with the KU Leuven, teaching electric power and energy systems. His research interests are within the framework of grids, smart grids, the deployment of all the new grid technologies and their integration with new resources and the demand in electricity. He is also Guest Professor at Imperial College of Science, Medicine and Technology, London, UK. Dr. Belmans is a Fellow of the IEEE and the IET. He is also the CEO of EnergyVille, the Executive Director of the Global Smart Grid Federation and Honorary Chairman of the board of Elia, the Belgian transmission grid operator.